2022 IEEE 25th International Conference on Intelligent Transportation Systems (ITSC)
October 8-12, 2022, Macau, China

Safety Critical Control of Mixed-autonomy Traffic via a Single Autonomous Vehicle

Jingyuan Zhou, Huan Yu

***Abstract*— Connected and automated vehicles (CAVs) have shown great potential in improving traffic throughput, stability, and safety in mixed-autonomy traffic. Many recent research studies focus on developing longitudinal control strategies for CAVs to achieve string stability of a heterogeneous vehicle platoon but the potential impact of these control strategies on safety has not been fully addressed. This paper proposed a safety-critical control strategy for CAV leading cruise control (LCC) framework in which there are both preceding and following human-driven vehicles (HDVs) for a single CAV. Considering the safety challenges brought by sudden acceleration and deceleration of the HDVs around the CAV, we introduced the notion of control barrier functions (CBF) to impart collision-free safety on a controlled LCC system. The safety of both HDVs and CAV are incorporated into the constraint-handling control design using a quadratic program, in which the actual CAV control input from a nominal input is penalized quadratically while the CBF safety constraints of control input guarantee the non-negative spacing between vehicles. The simulation results were conducted to validate the proposed control strategy for two safety-critical scenarios.**

I. Introduction

As vehicle-to-vehicle communication technology rapidly develops, using connected and automated vehicles (CAVs) to improve the efficiency and stability of the transportation system has been widely studied over the recent decades. Most existing studies focus on controlling a platoon of CAVs and its string stability, given different choices of information topology and formation geometry [8]. Early studies focused on adaptive cruise control (ACC) [10] that automatically adjusts the speed of vehicles to maintain a safe distance from the predecessor vehicle. Extended from ACC, as shown in Fig.1 (a), cooperative adaptive cruise control (CACC) [1], [12] assumed that all vehicles in a platoon are CAVs and developed linear feedback controller to mitigate disturbances in platoon [12]. Model predictive control (MPC) was used in [11] to guarantee safety distance between adjacent vehicles in the CACC framework.

Despite the promising future envisioned for fully connected and automated traffic systems, a long transition period is inevitable during which CAVs and human-driven vehicles (HDVs) have to coexist. Many recent research efforts are being put into mixed autonomy traffic where only a portion of vehicles are CAVs [5], [13], [14], [16], [18], [22], [23]. In [5], a single autonomous vehicle was used to stabilize the traffic flow. [13] demonstrated that the CAVs in mixed-autonomy traffic can dampen stop-and-go waves. The controllability and reachability of mixed-autonomy were studied by [22], which proved that a single CAV can stabilize traffic flow in the ring-road setting. Considering heterogeneous HDVs and communication abilities of CAVs, [16] proposed an optimal control control strategy [7]. The leading cruise control (LCC), as shown in Fig.1 (c), was firstly introduced in [14], in which the CAV control is designed to simultaneously adapt its motion to the preceding HDVs as well as to lead the following HDVS. The car-following behaviors are described with optimal velocity car-following model [4] and a linear feedback controller is designed for CAV acceleration control input. Furthermore, a data-driven approach to LCC is proposed by [15]. In this paper, we use the LCC framework to describe the longitudinal dynamics of mixed-autonomy, as the CAV's impact on both the downstream and upstream traffic flow is addressed with the framework. This paper focuses on developing a safety-critical CAV control strategy that guarantees both safety and string stability under the LCC framework.

Safety is of critical importance for traffic systems. Many studies focus on safety [9], [21] or string stability [5], [16], [22] as different objectives of mixed-autonomy traffic, but safety-critical control of mixed-autonomy traffic combining the two objectives has not been fully addressed. In particular, we investigate whether the control laws developed for CAVs to smooth traffic can guarantee the safety of the system and then develop a safety-enhanced control strategy using

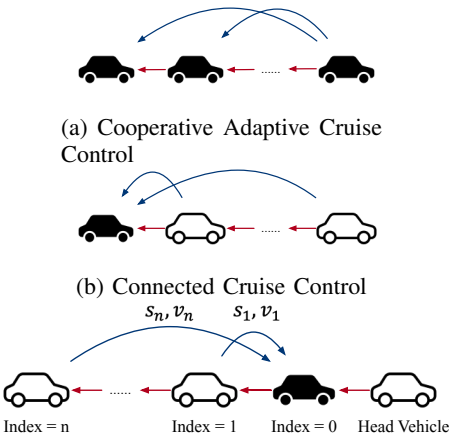

(a) Cooperative Adaptive Cruise Control

(b) Connected Cruise Control

(c) Leading Cruise Control

Fig. 1: Different control strategy framework for CAVs. The blue arrows represent wireless communication topology and the red arrows represent the interaction direction of HDVs. The white vehicles represent HDVs and the black vehicles represent CAVs. For leading cruise control (c), the CAV receive information from the head HDV and following HDVs.

Jingyuan Zhou and Huan Yu are with the Hong Kong University of Science and Technology (Guangzhou), Thrust of Intelligent Transportation, Nansha, Guangzhou, 511400, Guangdong, China. Huan Yu is also affiliated with the Hong Kong University of Science and Technology, Civil department, Hong Kong SAR, China. Email:*huanyu@ust.hk*

2022 IEEE 25th International Conference on Intelligent Transportation Systems (ITSC) | 978-1-6654-6880-0/22/$31.00 ©2022 IEEE | DOI: 10.1109/ITSC55140.2022.9921901

a single CAV to stabilize the traffic flow in a "collision-free" manner.

Safety of dynamical systems is usually approached by constraint-handling control methods such as classical optimal control, model predictive control, barrier Lyapunov function (BLF) [24] and control barrier function (CBF) [2]. Compared with the aforementioned approaches, the CBF control method provides a progressive approaching rate to the safety barrier which is a more realistic design for traffic acceleration control input. Moreover, neither MPC nor BLF contains the notion of a nominal controller like CBF control, which can be formulated for various primary control objectives, and only when the safety constraints are active, the control input need to deviate from the nominal controller. Therefore, we employ CBF with a nominal controller for LCC so that both string stability and safety can be achieved. The CBF has been applied in a wide range of safety-critical systems, including adaptive cruise control [3], multi-robot system [17], traffic merging [20]. However, to the best knowledge of the authors, using CBF for safety-critical control of LCC has not been studied before.

Specifically, we integrate a nominal feedback controller and CBF through a quadratic program (QP). The safety and string stability of the traffic flow in the LCC framework are simultaneously guaranteed when the safety constraints of the control barrier function are inactive. Only when the safety constraints are violated, the control input will deviate from the nominal controller. The CAV guarantees the safe spacing between all of its following HDVs and the HDV ahead of it. To construct the above-mentioned method, we formulate a quadratic program-based controller with CBF constraints and a feedback nominal controller [14]. Such a safety-critical control strategy can also be applied for other choices of control objectives beyond string stability, such as fuel consumption and CO2 emission.

II. LCC Model and nominal controller

In this section, the LCC modeling of mixed-autonomy traffic with a single CAV is introduced. We consider $n+2$ vehicles on a single lane road as shown in Fig.1 (c) and only longitudinal dynamics are considered. We briefly introduce the string stability and how it is guaranteed by nominal controller design [14], based on which the CBF safety design will be introduced.

A. Modeling of mixed-autonomy traffic

The mixed-autonomy traffic model constitutes two parts: the car-following model for human-driven vehicles and the model for CAV in which control input is designed.

For HDVs, the car-following dynamics are described with the ordinary differential equations (ODEs)

$$\dot{v}_i(t) = F\left(s_i(t), \dot{s}_i(t), v_i(t)\right), \tag{1}$$

where the acceleration of vehicle i is a function of its own velocity v_i, the space s_i between vehicle i and vehicle $i-1$ and the differential of space $\dot{s}_i(t)$. The equilibrium of the system $v^\star$ and $s^\star$ satisfy:

$$F\left(s^\star, 0, v^\star\right) = 0. \tag{2}$$

The nonlinear car-following model is linearized around the equilibrium.

$$\dot{\tilde{s}}_i(t) = \tilde{v}_{i-1}(t) - \tilde{v}_i(t), \tag{3}$$

$$\dot{\tilde{v}}_i(t) = \alpha_1 \tilde{s}_i(t) - \alpha_2 \tilde{v}_i(t) + \alpha_3 \tilde{v}_{i-1}(t), \tag{4}$$

where $\alpha_1 = \frac{\partial F}{\partial s}, \alpha_2 = \frac{\partial F}{\partial \dot{s}} - \frac{\partial F}{\partial v}, \alpha_3 = \frac{\partial F}{\partial \dot{s}}$ and the state variations of the ith HDV are defined as:

$$\tilde{s}_i(t) = s_i(t) - s^*, \tag{5}$$

$$\tilde{v}_i(t) = v_i(t) - v^*. \tag{6}$$

The optimal velocity model (OVM) [4] is chosen

$$F(\cdot) = \alpha\left(V\left(s_i(t)\right) - v_i(t)\right) + \beta \dot{s}_i(t), \tag{7}$$

where $V(s)$ is a continuous piecewise function, representing the spacing-dependent desired driving velocity function of the human driver. $V(s)$ is given by:

$$V(s) = \begin{cases} 0, & s \le s_{\mathrm{st}} \\ \frac{v_{\max}}{2}\left(1 - \cos\left(\pi \frac{s - s_{\mathrm{st}}}{s_{\mathrm{go}} - s_{\mathrm{st}}}\right)\right), & s_{\mathrm{st}} < s < s_{\mathrm{go}} \\ v_{\max}, & s \ge s_{\mathrm{go}} \end{cases} \tag{8}$$

where $s_{\mathrm{st}}, s_{\mathrm{go}}, v_{\max}$ represent a small spacing, a large spacing and the maximum velocity respectively. The coefficient α represents how the i-th vehicle accelerates with respect to its speed difference from the desired driving speed whereas coefficient β represents how the i-th vehicle changes its acceleration according to the speed difference from its leading vehicle. The coefficients relation between the OVM model (7) and the linearized model (3)(4) is given by: $\alpha_1 = \alpha \dot{V}\left(s^*\right), \alpha_2 = \alpha + \beta, \alpha_3 = \beta$.

For the CAV with $i = 0$, the vehicle dynamics can be written as (9) and (10), where the acceleration of the CAV is the control input $u(t)$.

$$\dot{\tilde{s}}_0(t) = \tilde{v}_h(t) - \tilde{v}_0(t), \tag{9}$$

$$\dot{\tilde{v}}_0(t) = u(t). \tag{10}$$

The state of the LCC model includes the space deviations and the velocity deviations of CAV and HDVs, given by

$$x(t) = \left[\tilde{s}_0(t), \tilde{v}_0(t), \ldots, \tilde{s}_n(t), \tilde{v}_n(t)\right]^T. \tag{11}$$

The linearized LCC model (3)(4) and (9)(10) is written as

$$\dot{x}(t) = Ax(t) + Bu(t) + D\tilde{v}_{\mathrm{h}}(t), \tag{12}$$

where $A \in \mathbb{R}^{(2n+2)\times(2n+2)}$, $B, D \in \mathbb{R}^{(2n+2)\times 1}$. The time-varying variable $\tilde{v}_{\mathrm{h}}(t)$ is the velocity deviation of the head vehicle, which is regarded as an external disturbance and $i, j \in [1, n]$,

$$A = \begin{bmatrix} P_1 & & & \\ P_2 & P_1 & & \\ & \ddots & \ddots & \\ & & P_2 & P_1 \end{bmatrix},$$

$$B = \left[b_0^T, b_1^T, \ldots, b_n^T\right]^T, D = \left[d_0^T, d_1^T, \ldots, d_n^T\right]^T,$$

$$P_1 = \begin{bmatrix} 0 & -1 \\ \alpha_1 & -\alpha_2 \end{bmatrix}, P_2 = \begin{bmatrix} 0 & 1 \\ 0 & \alpha_3 \end{bmatrix}$$

$$b_0 = \begin{bmatrix} 0 \\ 1 \end{bmatrix} b_i = \begin{bmatrix} 0 \\ 0 \end{bmatrix}, d_0 = \begin{bmatrix} 1 \\ \alpha_3 \end{bmatrix} d_j = \begin{bmatrix} 0 \\ 0. \end{bmatrix}$$

B. String stability and nominal controller

For a platoon of vehicles, head-to-tail string stability [6] is frequently used to evaluate the CAV's ability to attenuate velocity fluctuations of the following vehicles. Denote the velocity deviation of the vehicle at the head and the one at the tail as $\tilde{v}_{\mathrm{h}}(t)$ and $\tilde{v}_{\mathrm{t}}(t)$, respectively. The head-to-tail transfer function is defined as

$$\Gamma(s) = \frac{\widetilde{V}_{\mathrm{t}}(s)}{\widetilde{V}_{\mathrm{h}}(s)}, \tag{13}$$

where $\tilde{V}_{\mathrm{h}}(s), \tilde{V}_{\mathrm{t}}(s)$ denote the Laplace transform of $\tilde{v}_{\mathrm{h}}(t)$ and $\tilde{v}_{\mathrm{t}}(t)$, respectively. Then head-to-tail string stability holds if and only if

$$|\Gamma(j\omega)|^2 < 1, \quad \forall \omega > 0, \tag{14}$$

where $j = \sqrt{-1}$ and $|\cdot|$ denotes the modulus.

For the linearized LCC mixed-autonomy system (12), we consider a system with one preceding HDV of a single CAV and n following HDVs. The input and output of the LCC system are head vehicle velocity error $\tilde{v}_h(t)$ and tail vehicle velocity error $\tilde{v}_n(t)$. For HDVs dynamics (3)(4), the local Laplace transfer function is then written as:

$$\frac{\widetilde{V}_i(s)}{\widetilde{V}_{i-1}(s)} = \frac{\alpha_3 s + \alpha_1}{s^2 + \alpha_2 s + \alpha_1} = \frac{\varphi(s)}{\gamma(s)}. \tag{15}$$

where $\varphi(s) = \alpha_3 s + \alpha_1, \gamma(s) = s^2 + \alpha_2 s + \alpha_1$.

For the nominal controller of CAV, we adopt a state-feedback nominal controller proposed in [14], in which the CAV acceleration is constructed with the states of HDVs, as follows:

$$u_0(t) = \alpha_1 \tilde{s}_0 - \alpha_2 \tilde{v}_0 + \alpha_3 \tilde{v}_{-1} + \sum_{i \in \mathcal{F} \cup \mathcal{P}} \left(\mu_i \tilde{s}_i(t) + k_i \tilde{v}_i(t)\right), \tag{16}$$

where μ_i, k_i are the feedback gains corresponding to the state of vehicle i. The feedback control gains are chosen such that equation (14) is satisfied and the closed-loop system is string-stable. However, safety of vehicles are not considered, for example, the positive spacing between vehicles are not guaranteed in the closed-loop system.

Based on the nominal controller, we propose a control barrier function-quadratic programming-based controller design in which the conflict between safety and nominal stabilization is mediated by penalizing the deviation of the actual control input from the nominal controller quadratically.

III. Safe constraints and CBF-QP-based Controller

In this section, definitions of control barrier function and high-order control barrier function are first introduced, based on which the CBF-QP-based control design is developed. The safe constraints are designed for the safe space among the following HDVs and the safe space between the CAV and the head HDV. We then use quadratic programming to integrate safety conditions with the nominal controller. For feasibility consideration, we assign the safe space of the CAV and the head HDV with higher priority, than the one of the following HDVs.

A. Control Barrier Function

Consider an affine control system

$$\dot{x} = f(x) + g(x)u, \tag{17}$$

Where $\boldsymbol{x} \in \mathbb{R}^n$, $f : \mathbb{R}^n \to \mathbb{R}^n$ and $g : \mathbb{R}^n \to \mathbb{R}^{n \times q}$ are locally Lipschitz, $u \subset \mathbb{R}^q$. As for the system (12), $f(x) = Ax + H\tilde{v}_h$, $g(x) = B$.

Definition 1 (control barrier function [3]): Let $\mathcal{C} \subset D \subset \mathbb{R}^n$, $\mathcal{C} = \{x \in D \subset \mathbb{R}^n : h(x) \geq 0\}$ be the super level set of a continuously differentiable function $h : D \subset \mathbb{R}^n \to \mathbb{R}$, then h is a control barrier function for system (17) if there exists an class $\mathcal{K}$ functions α such that:

$$\sup_{u \in U} \left[L_f h(x) + L_g h(x) u\right] \geq -\alpha(h(x)), \tag{18}$$

for all $x \in D$.

For m^{th} order differentiable function $h : \mathbb{R}^h \to \mathbb{R}$, $m+1$ equations are defined:

$$\begin{aligned} \psi_0(x) :=& h(x), \\ \psi_1(x) :=& \dot{\psi}_0(x) + \alpha_1\left(\psi_0(x)\right), \\ &\vdots \\ \psi_m(x) :=& \dot{\psi}_{m-1}(x) + \alpha_m\left(\psi_{m-1}(x)\right). \end{aligned} \tag{19}$$

where $\psi_0 : \mathbb{R}^n \to \mathbb{R}, \psi_1 : \mathbb{R}^n \to \mathbb{R}, \psi_2 : \mathbb{R}^n \to \mathbb{R}, ..., \psi_m : \mathbb{R}^n \to \mathbb{R}$, $\alpha_1(\cdot), \alpha_2(\cdot), \ldots, \alpha_m(\cdot)$ denote m Class $\mathcal{K}$ functions.

CBFs are defined to impart system safety by guaranteeing forward invariance of a safe set of vehicle trajectories. The safe constraints defined by CBFs are constructed for system outputs. For a given nominal control input by CBF-QP, CBF constraints have relative degrees. Specifically, the safety constraints we proposed in this paper are spacing gaps of the following vehicles that are of high relative degree with respect to the control input. Therefore, high-order CBFs will be employed in our design.

Definition 2: (High-order CBF [19]) A function $h : \mathbb{R}^n \to \mathbb{R}$ is a high order control barrier function (HOCBF) of relative degree m for system (17) if there exist differentiable class $\mathcal{K}$ functions $\alpha_1(\cdot), \alpha_2(\cdot), \ldots, \alpha_m(\cdot)$ such that

$$\begin{aligned} &L_f^m h(x) + L_g L_f^{m-1} h(x,t) u + \tfrac{\partial^m h(x,t)}{\partial t^m} + O(h(x)) \\ &+\alpha_m\left(\psi_{m-1}(x)\right) \geq 0 \end{aligned} \tag{20}$$

for all $x \in C_1 \cap C_2 \cap, \ldots, \cap C_m$, $L_g L_f^{m-1} h(x) \in \mathbb{R}^{1 \times q}$. $O(\cdot)$ denotes the remaining Lie derivatives along f and partial derivatives with degree less than or equal to $m-1$.

$$\begin{aligned} C_1 :=& \{x \in \mathbb{R}^n : \psi_0(x) \geq 0\}, \\ C_2 :=& \{x \in \mathbb{R}^n : \psi_1(x) \geq 0\}, \\ &\vdots \\ C_m :=& \{x \in \mathbb{R}^n : \psi_{m-1}(x) \geq 0\}. \end{aligned} \tag{21}$$

The HOCBF are determined by a set of class $\mathcal{K}$ functions for constraints of high relative degrees. Similar with CBF, the safety set is forward invariant when the HOCBF is satisfied. Then we will introduce the design of the safety constraints.

B. Safety constraints design

HDVs safety constraint: Assume that there are n following HDVs, vehicle index $i \in [1, n]$. For the system (12), the spacing between the vehicle i and the preceding vehicle $i-1$ should be larger than a safe distance $s_{\text{safe,HDV}}$ so that

$$\tilde{s}_i + s^* \geq s_{\text{safe,HDV}}, \tag{22}$$

where the safe spacing of the following HDVs is defined as

$$s_{\text{safe,HDV}} = \tau_1(\tilde{v}_i - \tilde{v}_{i-1}), \tag{23}$$

and τ_1 is the HDV's reaction time.

We aim to design a CBF to guarantee the safety of the HDVs that follow the leading CAV. As the states of the following HDVs have a higher relative degree than the control input, we use HOCBF to tackle the problem. Consider the following HOCBF candidate for i-th following vehicle

$$h_i(x) = \tilde{s}_i + s^\star - \tau_1(\tilde{v}_i - \tilde{v}_{i-1}). \tag{24}$$

As presented in Definition 2, we choose K_α as a set of linear coefficients. The relative degree is i for the i-th following vehicles. To ensure the safety of the system (12) with respect to CBF candidate $h_i(x)$, the control input obtained by CBF-QP should satisfy:

$$\sup_{u \in U} \left[L_f^i h_i(x) + L_g L_f^{i-1} h_i(x) u \right] \geq -K_\alpha \eta_b(x), \tag{25}$$

where $L_f^i h_i(x) = \nabla h_i * (A * X)^r$, $L_g L_f^{i-1} h_i(x) = \nabla h_i * (A * X)^{i-1} * B$,

$$K_\alpha = [p_1, p_2, ..., p_i], \tag{26}$$

$$\eta_{h_i}(x) := \begin{bmatrix} h_i(x) \\ \dot{h}_i(x) \\ \ddot{h}_i(x) \\ \vdots \\ h_i^{(i-1)}(x) \end{bmatrix} = \begin{bmatrix} h_i(x) \\ L_f h_i(x) \\ L_f^2 h_i(x) \\ \vdots \\ L_f^{i-1} h_i(x) \end{bmatrix}. \tag{27}$$

CAV safety constraint: For safety of the leading CAV, its spacing to the head HDV needs to be guaranteed, considering the velocity disturbance from the head HDV. It is satisfied for the CAV:

$$\tilde{s}_0 + s^* - s_{\text{safe,CAV}} \geq 0, \tag{28}$$

where the safe space of CAV and head vehicle is defined as:

$$s_{\text{safe,CAV}} = \tau_2(\tilde{v}_0 - \tilde{v}_h), \tag{29}$$

and τ_2 denotes the reaction time of the velocity difference between CAV and head vehicle.

Consider the following CBF candidate

$$h_0(x) = \tilde{s}_0 + s^\star - \tau_2(\tilde{v}_0 - \tilde{v}_h). \tag{30}$$

As shown in Definition 1, we have the constraint for the control input:

$$L_f h_0 + L_g h_0 u + \alpha(h_0(x)) \geq 0, \tag{31}$$

where $L_f h_0 = -\tilde{v}_0 - \tau_2(\alpha_1 \tilde{s}_0(t) - \alpha_2 \tilde{v}_0(t))$, $L_g h_0 = -\tau_2$. The class $\mathcal{K}$ function $\alpha(x) = p_0 x$, where p_0 is a linear coefficient.

C. Quadratic Programming problem formulation

To guarantee the safety of the closed-loop LCC system, the control input u need to satisfy the proposed safety constraints, and at the the same time minimize deviations of u from the stabilizing nominal control input u_0. A quadratic programming yields that

$$u^* = \arg\min_u |u - u_0|^2, \tag{32}$$

where u_0 is the nominal controller (16). Assume that there are n following HDVs after CAV. The above QP problem is written as:

$$u^*(t) = \frac{1}{2} u(t)^T H u(t) + F^T u(t), \tag{33}$$

where $H = 1$, $F = -2u_0$, subject to:

HDVs$'$ safety constraint :

$$\begin{cases} L_f h_1(x) + L_g h_1(x) u \geq -K_\alpha \eta_b(x), \\ \vdots \\ L_f^n h_n(x) + L_g L_f^{n-1} h_n(x) u \geq -K_\alpha \eta_b(x), \end{cases} \tag{34}$$

CAV$'$s safety constraint :

$$L_f h_{CAV} + L_{g_2} h u + \alpha(h_0(x)) \geq 0. \tag{35}$$

Consider that the feasibility of the controller, HDVs safety constraints and CAV safety constraint may conflict in some conditions. In other words, the safety priority for the HDVs and CAV in the LCC framework needs to be defined. We set the CAV safety constraint with higher priority than the following HDVs safety constraint because if a collision happens for the leading CAV, a larger number of the following vehicles will be affected, compared with a collision in the following platoon.

IV. Numerical simulation

Simulation is carried out to validate performance of the proposed CBF-QP controller in two safety-critical scenarios.

A. Two safety-critical scenarios

We consider a simplified LCC setup that includes one head HDV, one CAV, and two following HDVs. The simulation is conducted using MATLAB *quadprog* to solve the quadratic programming problem. For initial condition, we assume that all vehicles in the platoon drive with equilibrium velocity $v^\star = 20$m/s and constant spacing $s^\star = 20$m. The simulation time step is 0.01s and the total simulation time is 50s. The model parameters of (8) are considered as: the small spacing $s_{st} = 5$ m, the large spacing $s_{go} = 35$ m, the maximum velocity $v_{max} = 40$ m/s and minimum velocity $v_{min} = 0$ m/s. The maximum acceleration and deceleration are set to 7 m/s^2 and -7 m/s^2 respectively. For the parameters of OVM (7), α and β are 0.6 and 0.9. The feedback gains of nominal controller in (16) and CBF parameters in (24)(25)(30)(31) are shown in the Table I.

We define a driving condition to be unsafe in which a collision happens (i.e. space gap is less than zero). For example, sudden acceleration/deceleration disturbances of HDVs last for a certain duration time. We set the disturbance acceleration from 0 m/s^2 to 7 m/s^2 and the disturbance deceleration from 0 s to -7 m/s^2. The disturbance duration

Feedback gains	μ_{-1}	k_{-1}	μ_1	k_1	μ_2	k_2
Value	0.2	-0.5	-0.2	0.05	-0.1	0.05
CBF parameters	τ_1	τ_2	p_0	p_1	p_2	
Value	4	3.5	12	1	0.85	

TABLE I: nominal control gains and CBF parameters

time is from 0s to 7s. For comparison, numerical simulations are conducted for the closed-loop LCC model with the nominal controller and with the CBF-QP-based controller respectively.

Two scenarios that could cause safety-critical failures for the LCC model are simulated. Consider the scenario 1, the HDVs following the CAV in the platoon may suddenly accelerate due to human mistakes caused by driving fatigue. Such an instantaneous acceleration could endanger the vehicles ahead of it. In particular, we add disturbances to the second following HDV which is at the tail of the platoon system. At 15s, the following HDV $(\text{index} = 2)$ accelerates with 7m/s^2 for 1.8s.

In scenario 2, the head HDV may brake abruptly to avoid a collision with some unexpected cutting-in vehicle or crossing pedestrians, which may jeopardize safety of the following vehicles. The disturbance signal is added to the head HDV in simulation. In particular, we consider an emergency at 35s that leads to the head HDV $(\text{index} = -1)$ decelerating with -7m/s^2 for 2s, and then the head HDV speed up to equilibrium speed for 2s after the risk is avoided.

B. Simulation results

To demonstrate the extent to which the safety of the platoon is improved, as shown in Fig. 2, the x-axis is the value of the disturbance signal (acceleration/deceleration), the y-axis is the duration time of the disturbance signal, the blue regions are the safety area of LCC using the nominal controller and the green regions are the expanded area by using the CBF-QP-based controller for LCC. In Fig. 2(a), the 2-nd following HDV's safety duration time increases by average 0.7s for the disturbance signal duration from 2m/s^2 to 7m/s^2. In Fig. 2(b), it can be seen that the safe region of the head vehicle is expanded by almost 60% using the CBF-QP-based controller. These simulation results prove that the CBF-QP-based controller can enhance the safety of both the CAV and the following vehicles.

For the case study of scenario 1, as shown in Fig. 3, we compare the effectiveness of the nominal controller and CBF-QP-based controller when there is a sudden acceleration of the following HDV. We give the following vehicle 2 a sudden acceleration at 15s, and Fig. 3(a) shows that the following vehicle 1 can not sense the vehicle behaviors behind so that the collision happens. However, Fig. 3(b) shows that the CAV using the CBF-QP controller ensures safety by speeding up the following HDV 1 and thus avoiding its collision with HDV 2.

The simulation results of scenario 2 are shown in Fig. 4, we compare the results of the nominal controller and CBF-QP based controller when the head vehicle has sudden deceleration. An emergency braking is added to the head vehicle at 35s. Fig. 4 (a) shows that even though the LCC using nominal feedback controller results in collision between the CAV and head vehicle as only the string stability of the platoon is considered. Fig. 4 (b) shows that the CBF-QP controller for CAV avoids such collision and thus improves the safety of the leading CAV with respect to the sudden braking event of the head vehicle.

To further illustrate the simulation results, we analyze the evolution of velocity and acceleration over the entire temporal simulation domain that includes both scenario 1 and scenario 2. In Fig. 5(b) and Fig. 6(b), we can see that the leading CAV's velocity and acceleration from 15.5s to 18s become much higher than that in Fig. 5(a) and Fig. 6(a), which means that the HOCBF constraints are active to prevent the collision between following HDV 1

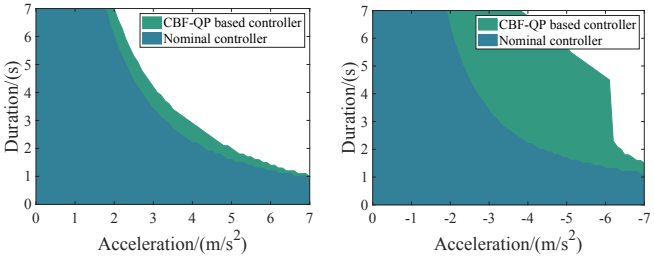

(a) Safety-critical scenario 1 (b) Safety-critical scenario 2

Fig. 2: Safety-guaranteed regions correspond to following vehicle acceleration disturbance of scenario 1 and head vehicle deceleration disturbance of scenario 2. The region colored in blue represents the safe region for the nominal controller with respect to disturbance amplitude and duration time. The region colored in green represents the additional safe area guaranteed by CBF-QP based controller.

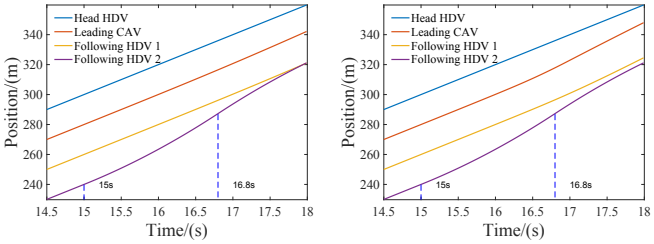

(a) Nominal controller (b) CBF-QP-based controller

Fig. 3: Trajectory comparison in safety-critical scenario 1

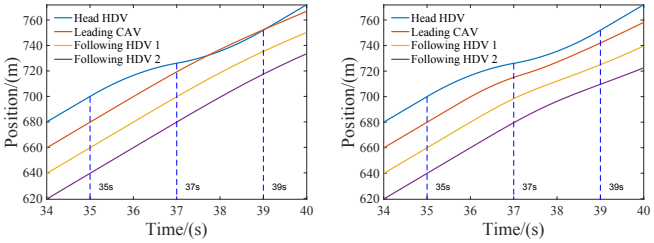

(a) Nominal controller (b) CBF-QP-based controller

Fig. 4: Trajectory comparison in safety-critical scenario 2.

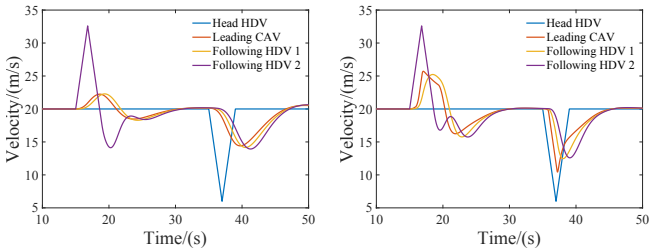

(a) Nominal controller (b) CBF-QP-based controller

Fig. 5: Velocity comparison for both scenarios.

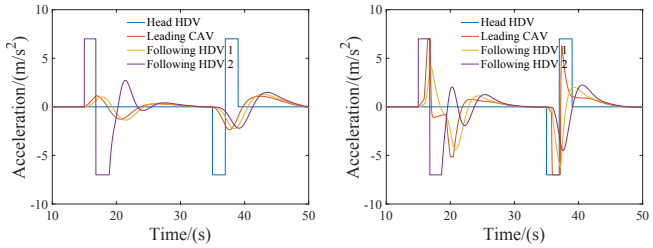

(a) Nominal controller (b) CBF-QP-based controller

Fig. 6: Acceleration comparison for both scenarios.

and following HDV 2. From 36s to 38s, the leading CAV decelerates using the CBF controller, avoiding collision in the same fashion.

V. CONCLUSION

In this paper, a CBF-QP-based CAV controller based on the leading cruise control framework is proposed to guarantee longitudinal collision-free safety of the mixed-autonomy traffic. The proposed CBF safety filter mediates the conflict between a nominal controller (string stability) and safety under disturbances using a QP. The leading CAV and the following HDVs are guaranteed to maintain safe spacing under head vehicle deceleration disturbance and under following HDV acceleration disturbance. For future work, addressing communication delays of state-feedback safety-critical control is of research interest.

REFERENCES

[1] Assad Alam, Ather Gattami, Karl H Johansson, and Claire J Tomlin. Guaranteeing safety for heavy duty vehicle platooning: Safe set computations and experimental evaluations. *Control Engineering Practice*, 24:33–41, 2014.

[2] Aaron D Ames, Samuel Coogan, Magnus Egerstedt, Gennaro Notomista, Koushil Sreenath, and Paulo Tabuada. Control barrier functions: Theory and applications. In *2019 18th European control conference (ECC)*, pages 3420–3431. IEEE, 2019.

[3] Aaron D Ames, Jessy W Grizzle, and Paulo Tabuada. Control barrier function based quadratic programs with application to adaptive cruise control. In *53rd IEEE Conference on Decision and Control*, pages 6271–6278. IEEE, 2014.

[4] Masako Bando, Katsuya Hasebe, Ken Nakanishi, and Akihiro Nakayama. Analysis of optimal velocity model with explicit delay. *Physical Review E*, 58(5):5429, 1998.

[5] Shumo Cui, Benjamin Seibold, Raphael Stern, and Daniel B Work. Stabilizing traffic flow via a single autonomous vehicle: Possibilities and limitations. In *2017 IEEE Intelligent Vehicles Symposium (IV)*, pages 1336–1341. IEEE, 2017.

[6] Shuo Feng, Yi Zhang, Shengbo Eben Li, Zhong Cao, Henry X Liu, and Li Li. String stability for vehicular platoon control: Definitions and analysis methods. *Annual Reviews in Control*, 47:81–97, 2019.

[7] Mihailo R Jovanović and Neil K Dhingra. Controller architectures: Tradeoffs between performance and structure. *European Journal of Control*, 30:76–91, 2016.

[8] Shengbo Eben Li, Yang Zheng, Keqiang Li, Yujia Wu, J Karl Hedrick, Feng Gao, and Hongwei Zhang. Dynamical modeling and distributed control of connected and automated vehicles: Challenges and opportunities. *IEEE Intelligent Transportation Systems Magazine*, 9(3):46–58, 2017.

[9] Haoji Liu, Weichao Zhuang, Guodong Yin, Rongcan Li, Chang Liu, and Shanxing Zhou. Decentralized on-ramp merging control of connected and automated vehicles in the mixed traffic using control barrier functions. In *2021 IEEE International Intelligent Transportation Systems Conference (ITSC)*, pages 1125–1131. IEEE, 2021.

[10] Greg Marsden, Mike McDonald, and Mark Brackstone. Towards an understanding of adaptive cruise control. *Transportation Research Part C: Emerging Technologies*, 9(1):33–51, 2001.

[11] Carlos Massera Filho, Marco H Terra, and Denis F Wolf. Safe optimization of highway traffic with robust model predictive control-based cooperative adaptive cruise control. *IEEE Transactions on Intelligent Transportation Systems*, 18(11):3193–3203, 2017.

[12] Vicente Milanés, Steven E Shladover, John Spring, Christopher Nowakowski, Hiroshi Kawazoe, and Masahide Nakamura. Cooperative adaptive cruise control in real traffic situations. *IEEE Transactions on intelligent transportation systems*, 15(1):296–305, 2013.

[13] Raphael E Stern, Shumo Cui, Maria Laura Delle Monache, Rahul Bhadani, Matt Bunting, Miles Churchill, Nathaniel Hamilton, Hannah Pohlmann, Fangyu Wu, Benedetto Piccoli, et al. Dissipation of stop-and-go waves via control of autonomous vehicles: Field experiments. *Transportation Research Part C: Emerging Technologies*, 89:205–221, 2018.

[14] Jiawei Wang, Yang Zheng, Chaoyi Chen, Qing Xu, and Keqiang Li. Leading cruise control in mixed traffic flow: System modeling, controllability, and string stability. *IEEE Transactions on Intelligent Transportation Systems*, 2021.

[15] Jiawei Wang, Yang Zheng, Qing Xu, and Keqiang Li. Data-driven predictive control for connected and autonomous vehicles in mixed traffic. *arXiv preprint arXiv:2110.10097*, 2021.

[16] Jiawei Wang, Yang Zheng, Qing Xu, Jianqiang Wang, and Keqiang Li. Controllability analysis and optimal control of mixed traffic flow with human-driven and autonomous vehicles. *IEEE Transactions on Intelligent Transportation Systems*, 22(12):7445–7459, 2020.

[17] Li Wang, Aaron D Ames, and Magnus Egerstedt. Safety barrier certificates for collisions-free multirobot systems. *IEEE Transactions on Robotics*, 33(3):661–674, 2017.

[18] Cathy Wu, Abdul Rahman Kreidieh, Kanaad Parvate, Eugene Vinitsky, and Alexandre M Bayen. Flow: A modular learning framework for mixed autonomy traffic. *IEEE Transactions on Robotics*, 2021.

[19] Wei Xiao and Calin Belta. High order control barrier functions. *IEEE Transactions on Automatic Control*, 2021.

[20] Wei Xiao, Calin Belta, and Christos G Cassandras. Decentralized merging control in traffic networks: A control barrier function approach. In *Proceedings of the 10th ACM/IEEE International Conference on Cyber-Physical Systems*, pages 270–279, 2019.

[21] Lanhang Ye and Toshiyuki Yamamoto. Evaluating the impact of connected and autonomous vehicles on traffic safety. *Physica A: Statistical Mechanics and its Applications*, 526:121009, 2019.

[22] Yang Zheng, Jiawei Wang, and Keqiang Li. Smoothing traffic flow via control of autonomous vehicles. *IEEE Internet of Things Journal*, 7(5):3882–3896, 2020.

[23] Wen-Xing Zhu and HM Zhang. Analysis of mixed traffic flow with human-driving and autonomous cars based on car-following model. *Physica A: Statistical Mechanics and its Applications*, 496:274–285, 2018.

[24] Yang Zhu and Feng Zhu. Barrier-function-based distributed adaptive control of nonlinear cavs with parametric uncertainty and full-state constraint. *Transportation Research Part C: Emerging Technologies*, 104:249–264, 2019.